euronoise 2021
25th to 27th of October
Madeira, Portugal - online

Acoustical shock waves interactions: Signal based determination of non-linearities

Samuel Deleu[1], Romain Gojon[1], Jérémie Gressier[1]

[1]ISAE-SUPAERO, Université de Toulouse, Toulouse, France
samuel.deleu@isae-supaero.fr
romain.gojon@isae-supaero.fr
jeremie.gressier@isae-supaero.fr

Abstract
The propagation of high amplitude acoustic waves can lead to non-linear effects including the focusing into shock fronts. The presence of discontinuities in acoustic signals interacting with simple geometries triggers non-linear behaviors. The present paper deals with the analysis of such acoustical shock waves, as it is mainly referred to in the literature, with the intent to identify and quantify non-linearities from a signal based point of view. This is a key issue to ensure the best source localization method when dealing with high amplitude or long range acoustics. While bearing computational efficiency in mind, extensions of classical linear equations for acoustics are commonly used to take into account non-linear acoustics. However, the following study will solve full Euler equations using high order spectral schemes and a compact limiter to improve the numerical solution accuracy of a propagated discontinuity. Two types of waveforms, i.e a basic step shock and a more acoustically relevant N-wave will be investigated to segregate and identify the different non-linear behaviors from several appropriate parameters.

Keywords: Nonlinear acoustics, Irregular reflection, Step shock, N-wave, High order Spectral differences.

1 Introduction

The localization of acoustic sources has an extensive interest for defense application. Impulse source signals are typically triggered from artillery shots from which two types of acoustic signals are identified: the Mach wave generated by the bullet displacement and the spherical shock wave generated by the muzzle blast. Both signals are strictly non-linear. Determining the non-linearity contribution in the localization process is of great importance. Source localization methods are usually based on the linear propagation of the sound which is a valid assessment whenever the pressure disturbance is several orders of magnitude lower than the ambient pressure. It can be the case in the musical industry or in studies such as Room and Building acoustics. However, when dealing with impulsive sound sources, non-linearities have to be taken into account. Time reversed acoustics [1] or ray tracing [2] have been widely used in the case of impulsive sound sources, without considering the influence of non-linear behavior on acoustical shock interactions with structures. The present study aims at identifying such non-linearities from a signal point of view in order to assess properly the influence of non-linear effects on the accuracy of the source localization or not. The signal based motivation comes from the will to assess such behaviors directly from measured signals that are commonly obtained using microphones.

Shock wave reflection onto rigid surfaces represents a fundamental domain of interest. This phenomenon has been theoretically investigated by von Neumann [3], although the experimental evidence was already performed by Ernst Mach [4] back in 1878. Ben Dor drew inspiration from these studies and gave a thorough analysis of the phenomenon in his book [5]. The incident and the reflected shocks, as they propagate along

the rigid surface, result in a reflection pattern which can be divided into two main types namely *regular* and *irregular*.

When a shock wave propagates over a solid wedge, the induced flow reacts with the surface in such a way that a second reflected shock is naturally generated. Indeed, the velocity induced by the passage of the shock remains perpendicular to the shock. However, the wedge being a perfectly rigid surface compels the local flow field behind the shock to remain parallel to the wedge. The easiest way for the flow to undergo such a change in direction is to go through a shock wave. Whenever the incident leading shock and the reflected shock share a point attached to the reflecting surface, the reflection is of type *regular* (RR). However, when the maximum flow turning angle at the given incident Mach number is less than the wedge angle, the reflected shock generated is unable to turn the induced flow back parallel to the wedge surface, causing the meeting point to detach from the reflecting surface: this is called *irregular reflection* (IR). The detached point is defined as the triple point in the case of strong shocks as it links the incident shock, the reflected shock and the Mach stem all together. The Mach stem is a discontinuity almost orthogonal to the surface that naturally occurs for the flow passing through both the incident and the reflected shock, to be of the same angle and pressure as the flow passing in between the triple point and the wedge surface, creating the flow condition for its appearance.

Theoretically, the prediction of such reflection regimes can be done using the Rankine-Hugoniot (RH) relations along with appropriate conditions to close the system of equations (3-Shock-Theory) [3]. This is valid for strong enough shockwaves. However, when dealing with acoustics, intensity is much lower – between a hundred of Pascal to a couple thousands – which leads to low acoustic Mach number values and different reflection patterns. The most important difference is the appearance of the von Neumann paradox. The latter states the discrepancy from the experimental evidence [6] of what resembles a Mach stem, that is not predicted by the theory for sufficiently weak shocks ($M_a < 0.47$) [7].

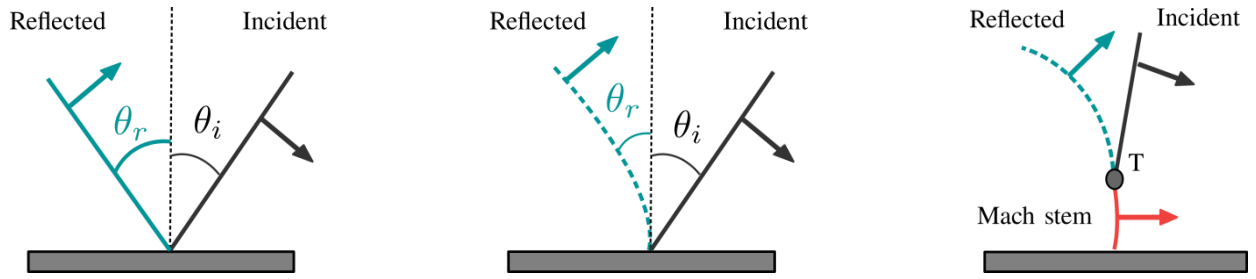

Figure 1 – Regime of reflections for plane acoustical shock waves
(a) Regular linear (b) Regular non-linear (c) von Neumann.

The consideration of a paradox is based on the assumption of a three-wave pattern. However, recent numerical studies [8] have shown that the condition for such reflection is the existence of a fourth wave, as Guderley already suggested back in 1947 [9]. Collela and Henderson [7] proposed the absence of an actual triple point with the reflected shock being spread out into a continuous wave before hitting the incident shock. Tesdall *et. al.* [10] provided an extended approach of the 2-D Burger equation expressed in self-similar coordinates aiming at improving the resolution obtainable near the triple point in weak shock reflections. They presented numerical evidence of a structure of reflected shocks and expansion waves coming from multiple triple points. This sequence of triple points induces a sequence of tiny supersonic regions behind the leading triple point in the case of an inviscid weak shock reflection. Supersonic patches occur over a region of the order of several thousandths of the total dimension of the perturbed flow which explains why it has only been observed numerically in recent history. The first ones to experimentally observe its presence were Skews and Ashworth [11] who carried out experiments on a large-scale so the region behind the triple point could be wide enough to be resolved. With better computational efficiency, finer simulation showed that the Guderley Reflection (GR), presenting a single supersonic patch structure, is

nothing else than an under resolved case of a reflection structure presenting a succession of supersonic patches and named Guderley Mach Reflection (GMR) resolving the paradox along the way [10].

As stated above, weak shocks have been largely studied. The term acoustical shock was first introduced by Keller [12] in 1954. Acoustical shocks are defined by their acoustic Mach number which is the ratio of the peak particle velocity over the ambient sound speed $M_a = \frac{u_a^{max}}{c_0}$ [13] which in the case of plane wave can be expressed as a function of the acoustic pressure $p_a = P - P_0$: $M_a = \frac{p_a^{max}}{\rho_0 c_0^2}$ with ρ_0 the ambient density, c_0 the ambient sound speed and p_a^{max} the maximum peak pressure amplitude of the incident shock. Peak pressure is a common term regarding oscillating signals. It has been decided in this study to take the step value as the maximum peak pressure when dealing with step shocks. Typical values for acoustical shocks are for $M_a < 0.05$ [14].

Acoustical shocks can emerge from various ways. Non-linearity through speed of sound shifts makes the wave locally focus or expand along with compression or expansion respectively. This effect is strengthened with the wave amplitude and the distance of propagation. The signal can also be discontinuous from the start with a low amplitude discontinuity such as a bullet Mach wave, a sonic boom or an electric spark source sound signature [15].

The study is composed as follows: the numerical setup is presented in section 2 including the mesh definition, the solver and the limiter description; section 3 focuses on the comparison of preliminary simulation results for the reflection of a step shock and an N-wave onto a wedge singularity; results are compared against available numerical results [16] in order to validate the numerical approach; section 4 describes the different parameters adopted to identify acoustical shock wave reflection non-linearities from two different wave topologies namely the step shock and the N-wave.

2 Mesh definition and Numerical Setup

The propagation of acoustical shock waves onto rigid corners is performed using an in-house solver: IC3. This solver is a massively parallel high-order computational code based on the use of unstructured meshes and aimed at solving the three-dimensional Navier-Stokes equations with explicit time integration. However, the scope of this study is limited to full Euler equations. Spectral difference (SD) scheme being intrinsically low dissipative, it is a consistent choice when dealing with acoustic propagation. Its stencil compactness induces good HPC capabilities, important whenever unstructured mesh is adopted.

The SD schemes have been implemented in IC3 [17] along with a compact spectral limiter SWeP (Spatially Weighted Projections) [18] specially developed for the propagation of discontinuities. To our knowledge, this is the first time an SD scheme is used for the simulation of the propagation of acoustical shocks. A fundamental result of solving non-linear equations using polynomial approximation is the apparition of spurious oscillations at the discontinuity. The main purpose of the limiter lies in the inhibition of those oscillations that are usually responsible for unwanted noise in the solution as well as computation failure in some cases. To do so, the general strategy deployed here is to project the solution on a reduced order base of polynomials whenever a discontinuity is detected. The discontinuity detection strategy is based on the one developed by Persson for artificial viscosity [19]. The limitation procedure is then applied to any detected cell bearer of discontinuity to apply the local polynomial reduction and damp the unwanted oscillations. More specifically numerical simulations were carried out using the third-order SD scheme which means that each cell contains 3x3 solution points. The solution is updated at a fixed time step – $dt = 5.10^{-8}s$ for step shocks and $dt = 2.1.10^{-7}s$ for N-waves – using a third order Runge-Kutta scheme. The values were chosen to respect a CFL condition for spectral schemes: $c_0 \frac{dt}{dx}(p+1) < 1$ with p the order of the polynomial. Regarding the mesh, we use a 1300x400 2-D grid constructed with an automated tool which transforms an

orthonormal cartesian mesh into a mesh adapted to our problem through a bijective analytical function. This simple geometry is an asset for the database construction (see 3.1.1) since it is flexible enough to run multiple simulations with different values for the wedge angle θ_w.

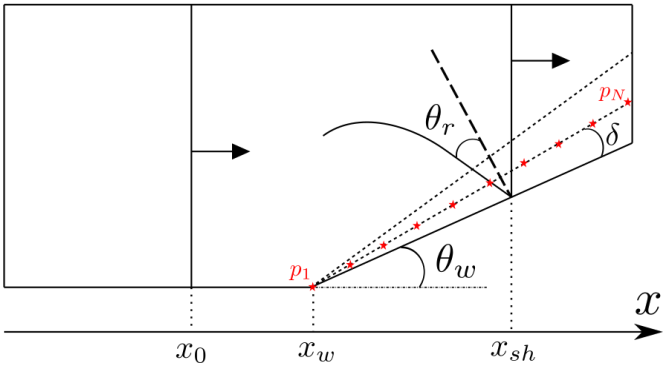

Figure 2 – 2-D domain scheme with probes positions x_{probe} indicated along a line δ.

Figure 2 illustrates the domain general form along with the different numerical probes we used to obtain pressure signals over time, as a microphone would give on a real life application. Ten probes are arranged along a line which makes an angle δ with the reflecting surface. We chose $\delta \in [0°, 20°]$. The shock initially located at $x_0 = 0{,}3m$ propagates in a steady environment with $P_0 = 1.0 \times 10^5 Pa$. The left inflow conditions are calculated as the downstream flow behind the incident shock using the RH relations for a planar shock wave moving at a prescribed velocity W_s,

$$W_s = c_0 \sqrt{M_a \frac{\gamma+1}{2} + 1} \tag{1}$$

where M_a is the acoustic Mach number, γ the heat capacity ratio and c_0 the ambient sound speed.

The same configuration is used for the initialization of the N-wave without the left boundary condition.

3 Results

The computed solutions are presented in the next section for both investigated wave topologies namely the step shock and the N-wave. The intent is to validate the simulations and to present the numerical databases created.

3.1 Step Shock

A step shock is not a proper acoustical waveform since acoustical shocks are always preceded or followed by non-constant flow which modifies the reflection structure. However, step shock reflections have been widely studied and constitute a simple case to investigate acoustical shocks interaction with corners.

3.1.1 Database Construction

The shock wave reflection is controlled with the strength of the shock and the geometry of the obstacle it hits. We wish to assess and reproduce every reflection pattern available on given ranges of acoustic Mach number and wedge angle that are relevant for acoustical shocks. Wedge angle range is chosen to be near the validity of the transition criteria a deduced from paraxial approximation equations [20]. For specific values

of this parameter given Table 1, different reflection patterns occur. Urban source localization would favor ground reflections whenever it comes to monitor such acoustical shocks. This assumption presumes that wide angle reflections are less likely to happen which is the reason why large angle values are left aside in this study but is currently under investigation. Eventually we chose $M_a \in [0.0005, 0.1]$ and $\theta_w \in [2°, 35°]$.

3.1.2 Preliminary Results and Literature Comparison

In their thorough numerical analysis, Baskar and Coulouvrat [16] suggested critical values of the parameter a in the case of a step shock for the transition from one reflection regime to another (see description of said parameter Table 1).

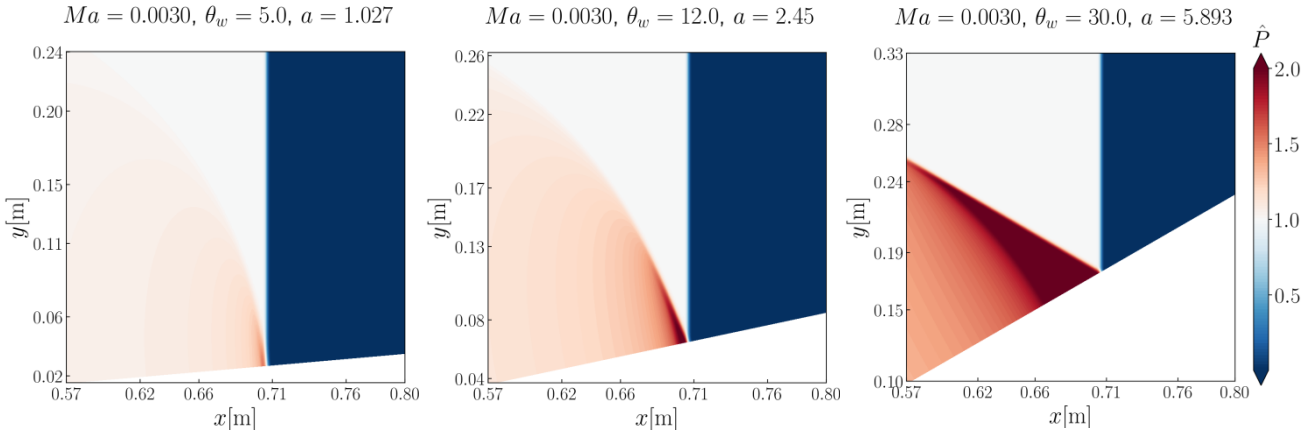

Figure 3 – Reflection regime transitions for Ma = 0.003
a) von Neumann Reflection b) Non-linear Regular Reflection c) Linear Regular Reflection.

Results on Figure 3 were obtained with the same value of acoustic Mach number M_a. Only the wedge angle θ_w variations are responsible for the different reflection patterns. Figure 3.a) indicates a von Neumann reflection: incident and reflected shock meet above the reflecting surface, with the presence of a Mach stem acknowledging the irregular behavior. On the contrary, Figure 3.b) and 3.c) see their point of reflection well attached on the surface which leads to claim both reflections are regular. The angle of incidence is different from the angle of reflection on Figure 3.b), on the contrary to Figure 3.c) where they are equals. This leads us to segregate 3.b) from 3.c) and introduce two sub-categories amongst regular reflections: regular non-linear and regular linear respectively. The numerical results shown on Figure 3 are in good agreement with what is expected considering the reflection nature of a step shock.

Table 1 – Different acoustical shock reflection regimes according to the value of the critical parameter a [16], with θ_w the wedge angle, γ heat capacity ratio and M_a the acoustic Mach number.

Reflection type	Regime	Values for $a = \frac{sin(\theta_w)}{\sqrt{\frac{\gamma+1}{2}M_a}}$
Classical Snell Descartes	Regular Linear	$a > 5$
Generalized Snell Descartes	Regular Non Linear	$\sqrt{2} < a < 5$
Von Neumann Reflection	Irregular (Non Linear)	$a < 0.4$

3.2 N-Wave

DuMond *et al.* [21] investigated the dependence of the amplitude and period of the N-wave with the miss distance (nearest approach) of the bullet's trajectory and the microphone. They also helped theorize the formation, amplitude and duration of the N-wave, along with Landau [22]. The idealized N-wave consists of

a sharp positive pressure wave front that decays linearly to a rarefaction equally far below atmospheric before an abrupt return to atmospheric pressure. This wave topology is more relevant regarding acoustic propagation.

3.2.1 Database Construction

From experimental measures [23] and ballistic assumptions made from Whitham formula [24], we were able to set a range in amplitude that fits with the characteristic amplitude levels a microphone could experience in an urban environment for the detection of acoustical shock waves. The front shock and "tail discontinuity" [21] pressure levels of an N-wave being equal in absolute, states the symmetrical character of the N-wave studied here. In reality, it appears that the positive length is often greater than the negative part. The maximum pressure levels have been measured around 7000 Pa from the muzzle blast for a distance of 1m of an AK-47 [23] as well as from the Mach wave of a bullet of an AK-47 from a 300m shot distance and a miss distance of 25m which is around 100 Pa in amplitude [25]. Regarding those experimental values, the range for our N-wave numerical study has been set to $50\,Pa < p^f_{max} < 8000\,Pa$ with p^f_{max} being the peak pressure of the N-wave leading shock front. We used the RH relations for the shock and unsteady Riemann invariant along C- for the expansion fan to propagate the shock towards the preferred direction (from left to right).

3.2.2 Preliminary Results and Literature Comparison

As previously stated, values of a below 1.414 should lead to an irregular reflection for step shocks. However we can observe on Figure 4.a) that the reflection is regular non-linear as the reflected shock is curved and the reflecting point is attached to the surface, even though $a = 1.035$. The limit of the transition between regular and irregular reflection appears to be smaller for an N-wave than for a step shock. This behavior is backed up by Baskar numerical analysis [16] as well as Karzova's experimental study [15]. Both suggested a lower value of a for the transition: 0.8 and 1.05 respectively. The difference being that Karzova's N-waves were cylindrical whereas Baskar used plane N-waves which is the same as in this study.

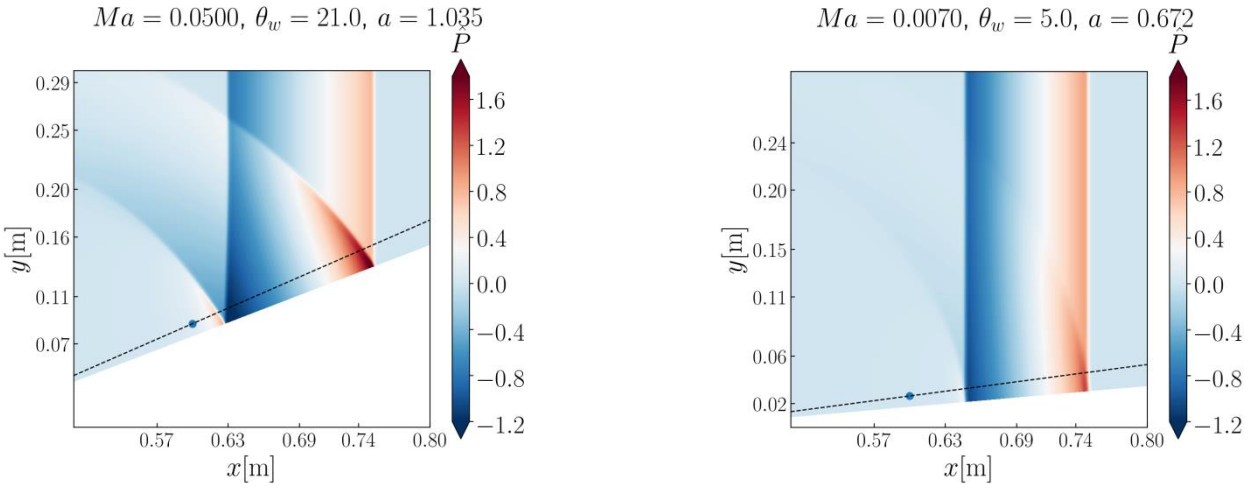

Figure 4 – Different N-wave reflection regimes:
a) Non-linear Regular Reflection b) von Neumann Reflection.

4 Signal Based Non-linearities Identification from Different Wave Topologies

Although the transition criterion gives an indication on the potential non-linearity of a reflection, we wish to investigate other potential criteria relevant enough to assess non-linearities.

4.1 Step Shock

The signal based analysis is performed on pressure time signature series. The theoretical value of the pressure behind a given shock P_i^{th} can be determined through RH relations for a plane wave. We define the normalized pressure $\hat{P}$ such as:

$$P_i^{th} = \left[(M_s^2 - 1)\frac{2\gamma}{\gamma+1} + 1\right]P_0 \text{ and } \hat{P} = \frac{P-P_0}{P_i^{th}-P_0}. \quad (2)$$

Where M_s is the shock Mach number, γ the heat capacity ratio and P_0 the ambient pressure.

Behind the incident shock, $\hat{P} = 1$, whereas behind the reflected shock, $\hat{P} = 2$ in the case of a regular linear reflection as stated from the theory. The color-map presented in Figure 5.a) has been constructed from the recorded signal of a given numerical probe located in the domain (see Figure 2). Here, $\delta = 5.1°$ and $x_{probe} = 0{,}6m$. The color-map illustrates the relative gap of the maximum value of $\hat{P}$ for each couple (M_a, θ_w), from the theoretical value that should be obtained in the case of a regular linear reflection. Black lines on Figure 5.a) represent the limits of the parameter a presented in Table 1. We can observe that $(M_a,\ \theta_w)$ leading to values of a above 5 respects the criteria as their color is close to the white shade representing the theoretical value of $\hat{P} = 2$. In the same region, the slight tendency for extremely low M_a to reach values of $\hat{P}$ above 2 is due to oscillations of the solution that peak at a maximum higher than $\hat{P} = 2$. Any gap from that theoretical value of 2 is a proof of a non-linear behavior for the reflected shock, as illustrated on Figure 5.b).

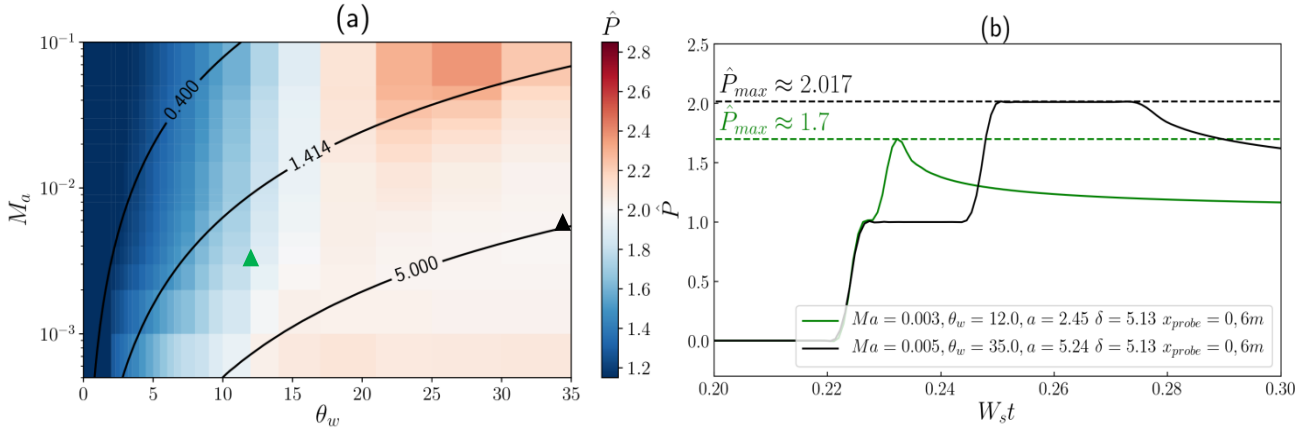

Figure 5 – a) Color-map of the parameter $\hat{P}$ for the stepshock database along with the theoretical limit values of a for the reflection transition (black lines) ; b) Corresponding pressure-time profiles of a linear regular reflection (black) and a non-linear regular reflection (green).

4.2 N-Wave

The expansion behind the leading shock of an N-wave decreases intensity as shown in the shift of the transition limit between regular and irregular reflection. Because of this unsteady state, the pressure behind the reflected shock of a regular linear reflection does not reach the expected value of 2 (Figure 7) such as the ideal case of a step shock. Also, the competition between the pressure flow field behind the reflected leading shock and the expansion fan, deprives the latter from leading the rear shock back to its maximum negative amplitude; as it is the case before any interaction. This leads the absolute maximum value for the rear shock (Figure 6.a)) to remain lower than the maximum values for the front shock on the whole domain (Figure 6.b)). However, when looking at the pressure differences on Figure 7 (blue), the rear shock undergoes the biggest gap. This is due to the over-pressure right behind the reflected rear shock that can be seen as a little bump above 0. We noticed here that over-pressure happens for every couple $(M_a,\ \theta_w)$ regardless of whether it is linear or non-linear.

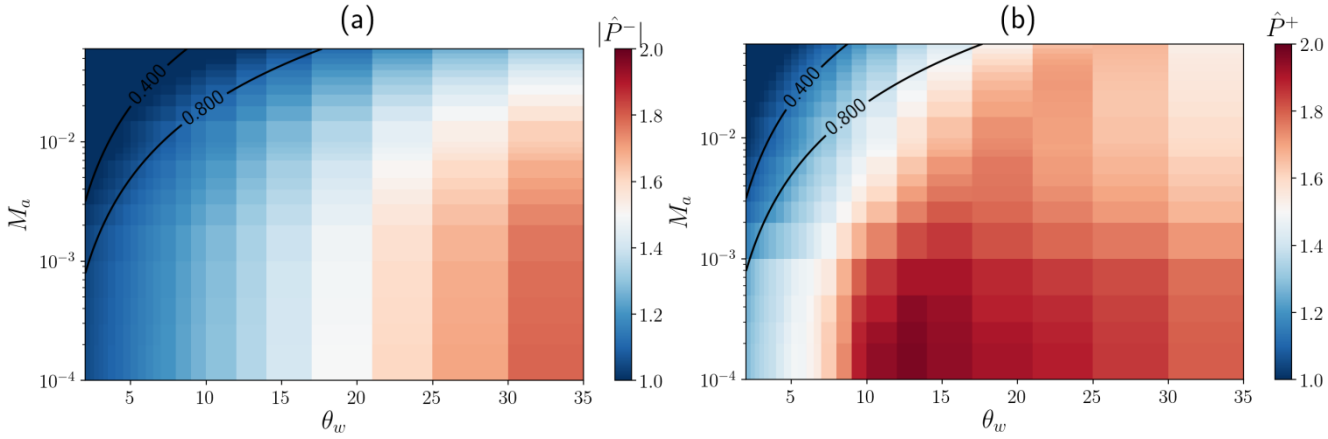

Figure 6 – Color-map of a) the absolute maximum of the rear shock $|\hat{P}^-|$; b) the maximum pressure of the leading shock $\hat{P}^+$; along with reflection transition limit (black lines) from [16] are plotted on both a) and b).

In the case of non-linear reflections (Figure 7 blue, Figure 9.a)) the bump seems confounded with the reflected rear shock. The tail discontinuity reflection is no longer competing with the expansion of the N since it happens behind the N, in a steady environment. Therefore, the pressure jump of the reflected shock is higher. Also, the rear shock has an absolute value smaller than the leading shock (as seen on Figure 6.b)). The combination of those two factors indicates that, across the reflected rear shock, the flow undergoes a local over-pressure greater than the difference between P_0 and the pressure behind the incident rear shock, hence the overshoot of P_0 behind the rear reflected shock.

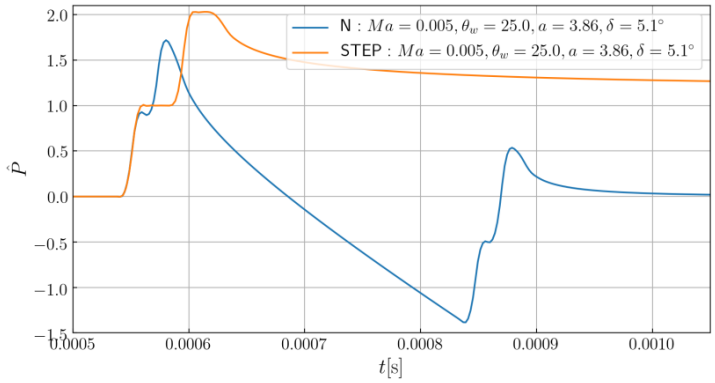

Figure 7 – Time pressure profiles for N wave (blue) and step shock (gold).

In the case of linear reflections (Figure 9. a) blue), the over-pressure is distant from the rear reflected shock. It can be seen as a third bump. The visible structure Figure 9.c) resembles what Baskar and Coulouvrat [16] named secondary reflected shock. The self-similarity of the step shock does not apply in the case of an N-wave and a dynamic transition occurs from irregular reflection back to regular reflection for sufficiently long range propagation. This inverted transition induces the rear triple point to hit back the rigid surface. According to Baskar *et. al* [16], it is supposed to be at the origin of the secondary reflected shock. Even though the shock structure they observed is very similar to ours, no transition occurred for the reflected rear shock since it is linear from the moment it interacts with the wedge.

In order to assess the non-linearity of an N-wave interaction with a wedge, the statistical distribution of the signal is analyzed. More specifically, the skewness of the signal distribution is evaluated. First, the time pressure signal obtained for a given probe (Figure 1) is truncated in a consistent way so that the N-shaped part of the signal is isolated (Figure 9.a)). This treatment skips the ambient pressure value from the distribution. Then, we calculate the skewness of our N-shaped distribution in order to estimate whether its interaction with a wedge induces a notable difference. A positive skewness would indicate that the negative pressure length is greater than the positive as the right tail of the distribution would be longer than the left thus indicating a possible non-linear behavior. Positive pressure values are located on the left side of our N-wave pressure profile. Negative skewness would indicate the reverse interpretation. Results are displayed on Figure 8.a) where skewness values μ_3 are referenced from around -0.36 to +0.36. On Figure 8.b), the quantity $\hat{P}^+ - |\hat{P}^-|$ is plotted. Its behavior is analogous to the skewness. From the skewness color-map, we can evaluate 6 different regions according to their values as shown on Figure 8.a).

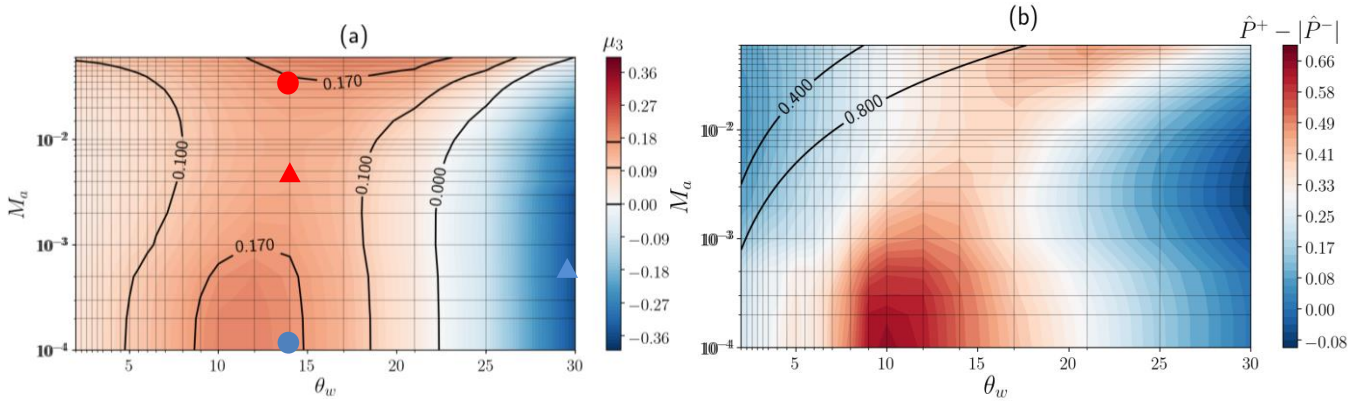

Figure 8 – Values for the N-wave from signal recorded at $\delta = 5.1°$ and $x_{probe} = 0{,}6m$:
a) Skewness μ_3 ; b) $\hat{P}^+ - |\hat{P}^-|$.

Figure 9 displays the time pressure profiles of two of those six regions (triangles) that have a different skewness value, $\mu_3 < 0.1$ and $0.1 < \mu_3 < 0.17$. High positive skewness values are located in two specific areas. One at high M_a (red circle), the other at low M_a (blue circle), but both for moderate angles around θ_w =15°. Truncated pressure signals as well as their corresponding histograms and pressure contours from which the skewness color-map is drawn can be found on Figure 9 and 10. In the low M_a area, the time-pressure signal (blue) can be divided into three zones: leading shock interaction, expansion fan and rear shock interaction. Two bumps can be observed in the first part; the smallest one being the incident leading shock front and the second one the reflected shock. In between, a pressure decrease expresses the interaction with the expansion fan. The same behavior happens for the rear shock. The presence of a decreasing plate between incident and reflected shock is noticeable on the histogram distribution for values at -0.5 and 1. In the second high skewness value area however, the signal (red) does not show the presence of any reflected shock for both leading and rear shock interaction. This is because irregular reflection happens in that case. The probe location being below the triple point, as illustrated with a blue dot on Figures 10, the signal is logically constituted of a single leading shock front and a single rear shock. The noticeable wavelength

difference between red and blue is mainly due to the non-linear propagation of the N-wave that tends to spread out as the front shock speed is travelling at a supersonic velocity $c + u$ and the rear shock speed at a subsonic velocity $c + u$. The higher the Mach number, the further the spread for a given measuring probes location.

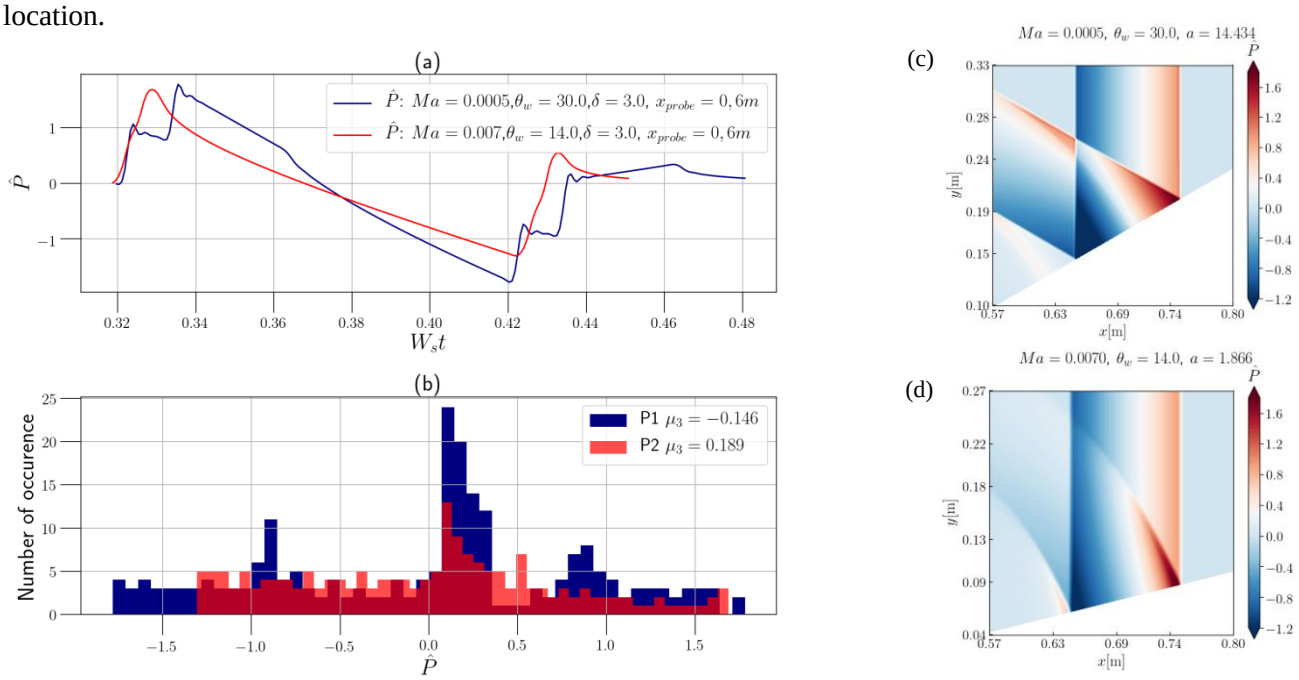

Figure 9 – Triangle zones: Time pressure profiles (a), corresponding histograms (b) and pressure fields (c,d).

As shown above (Figure 8.a)), maximum skewness values occur for two different wave profiles and two different reflection regimes, linear and non-linear. Even though the skewness parameter gives information on the reflection structure, it is not well suited for the evaluation of non-linearity provoked by the corner interaction.

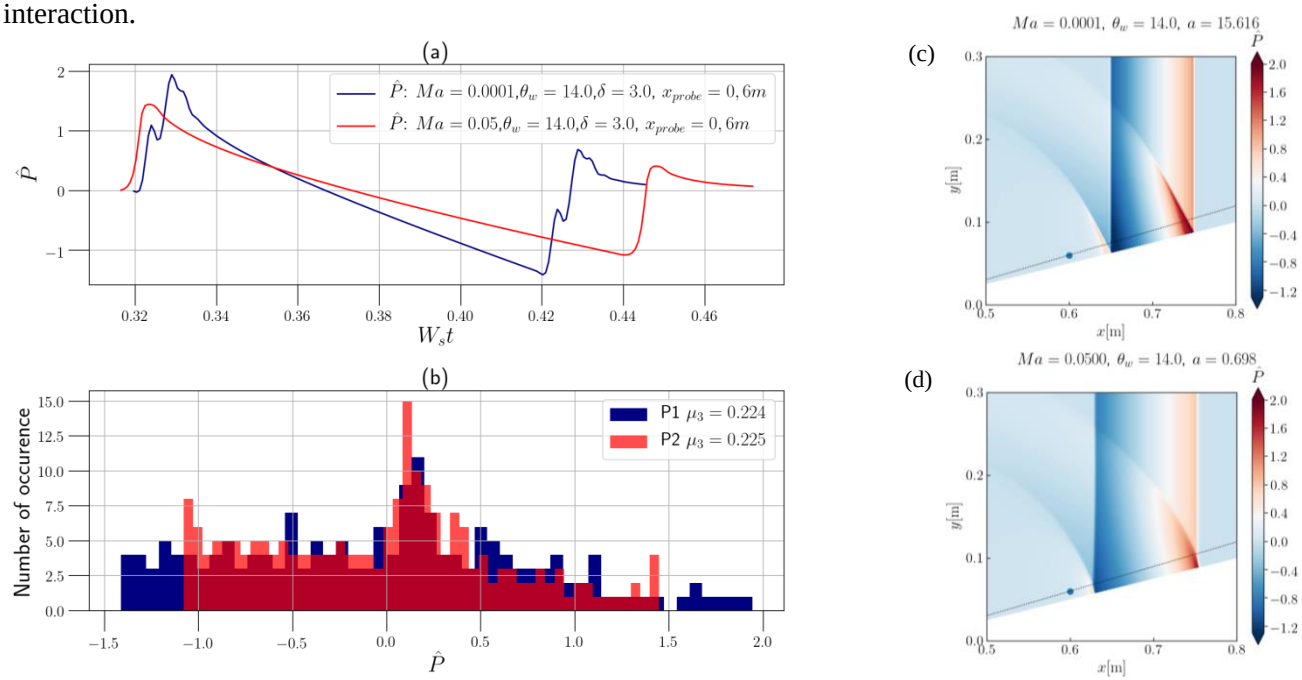

Figure 10 – Circle zones: Time pressure profiles (a), corresponding histograms (b) and pressure fields (c,d).

5 Conclusions

From the full Euler equation solved using spectral difference scheme, the reflection of an acoustical shock wave onto a rigid corner is numerically investigated. In particular, the analysis of signals for step shocks and N-wave is performed thanks to the construction of a database to cover an acoustically relevant range in the (M_a, θ_w) domain. The comparison of our numerical results with existing results from the literature shows a good agreement with what is expected. It has been shown that a well suited parameter to identify the presence of non-linearities in the case of a step shock is the evaluation of the maximum pressure of the measured signal. For N-wave topology, the signal distribution is investigated with the evaluation of the signal skewness in the entire (M_a, θ_w) domain. The results are mitigated regarding the efficiency for this parameter to segregate non-linear behavior and need further investigation.

Acknowledgements

The authors would like to thank the AID for their financial support and for permitting the publication of the research. This work was performed using HPC resources from GENCI-IDRIS and GENCI-CINES on Jean Zay, Occigen (Grant A0102A07178) and CALMIP on Olympe (Grant 2021-p1425).

References

[1] Cheinet, S., Ehrhardt, L., Broglin, T. Impulse source localization in an urban environment: Time reversal versus time matching. *The Journal of the Acoustical Society of America*, 139(1), 2016, pp 128-140.

[2] Scott, J. F., Blanc-Benon, P., Gainville, O. Weakly nonlinear propagation of small-wavelength, impulsive acoustic waves in a general atmosphere. *Wave Motion*, 72, 2007, pp 41-61.

[3] Von Neumann, J. “See Collected works”. In :Pergamon6, 1943.

[4] Mach, E. Über den Verlauf von Funkenwellen in der Ebene und im Raume, Sitzungsbr. Akad. Wiss. Wien 78, 1878, pp 819–838.

[5] Ben-Dor, G. *Shock Wave Reflection Phenomena*. Springer, . Second Edition, 2007.

[6] Bleakney, W.; Taub, A. H. Interaction of shock waves. *Reviews of Modern Physics*, 21(4), 1949, pp 584-605.

[7] Colella, P. and Henderson, L. F. The von Neumann paradox for the diffraction of weak shock waves, *J. Fluid Mech*, 213, ., 1990, pp 71–94.

[8] Tesdall, A. M.; Sanders, R. and Popivanov, N. Further Results on Guderley Mach Reflection and the Triple Point Paradox. *Journal of Scientific Computing*, 64(3), 2015, pp 721-744.

[9] Guderley, K. *Considerations on the structure of mixed subsonic-supersonic flow patterns*. Tech. Rep. F-TR-2168-ND. Wright Field 1947.

[10] Tesdall, A. M.; Hunter, J. K. Self-Similar Solutions for Weak Shock Reflection. *Society for Industrial and Applied Mathematics*, 63(1), 2002, pp 42-61.

[11] Skews, B. W.; Ashworth, J. T. The physical Nature of Weak Shock Wave Reflection *J. Fluid Mech.*, vol. 542, 2005, pp 105–114.

[12] Keller, J. B. Geometrical acoustics. I. The theory of weak shock waves. *Journal of Applied Physics*, 25(8), 1954, pp 938-947.

[13] Hamilton, M. F.; Blackstock, D. T. *Nonlinear Acoustics*. Acoustical Society of America, Second Edition, 2008.

[14] Yuldashev, P.; Karzova, M.; Khokhlova, V.; Ollivier, S.; Blanc-Benon, P. Mach-Zehnder interferometry method for acoustic shock wave measurements in air and broadband calibration of microphones. *The Journal of the Acoustical Society of America*, 137(6), 2015, pp 3314-3324.

[15] Karzova, M. M., Lechat, T., Ollivier, S., Dragna, D., Yuldashev, P. V., Khokhlova, V. A., & Blanc-Benon, P. Irregular reflection of spark-generated shock pulses from a rigid surface: Mach-Zehnder interferometry measurements in air. *The Journal of the Acoustical Society of America*, 145(1), 2019, pp 26-35.

[16] Baskar, S., Coulouvrat, F., Marchiano, R. Nonlinear reflection of grazing acoustic shock waves: unsteady transition from von Neumann to Mach to Snell–Descartes reflections. *Journal of Fluid Mechanics*, 575, 2007, pp 27-55.

[17] Lamouroux, R.; Gressier, J.; Grondin, G. A High-Order Compact Limiter Based on Spatially Weighted Projections for the Spectral Volume and the Spectral Differences Method. *J Sci Comput* 67, 2016, pp 375–403.

[18] Saez-Mischlich, G. High order numerical methods for unstructured grids and sliding mesh, *PhD Thesis*, 2021.

[19] Persson, P. O. Shock capturing for high-order discontinuous Galerkin simulation of transient flow problems. *21st AIAA Computational Fluid Dynamics Conference*, 2013.

[20] Zabolotskaya, E. A. Quasi-plane waves, in the nonlinear acoustics of confined beams. Sov. Phys. Acoust., 15, 1969, pp 35-40.

[21] DuMond, J. W. M., E. R. Cohen, W. K. H. Panofsky, and E. Deeds. Wave Forms and Laws of Propagation and Dissipation of Ballistic Shock Waves, *Journal of the Acoustical Society of America*, 18 (1), 1946, pp 97–118.

[22] Landau, L. D. On shock waves at large distances from the place of their origin. *J. Phys. USSR*, vol. 9, no 6, 1945, pp 496-500.

[23] Rasmussen, P.; Flamme, G.; Stewart, M.; Meinke, D.; Lankford, J. Measuring Recreational Firearm Noise, *Sound & Vibration*, 2009, pp 14-18.

[24] Whitham, G. B. *Linear and nonlinear waves*, Vol. 42, John Wiley & Sons, 2011.

[25] Cheinet, S.; Broglin, T. Sensitivity of shot detection and localization to environmental propagation. Applied Acoustics, 93, 2015, pp 97-105.